




# Spectroscopic ellipsometry to precisely estimate the thickness for optimizing the performance of three-layer broadband transparent electrodes

Keh-Moh Lin<sup>1,\*</sup>  and Swapnil Shinde<sup>1</sup>

<sup>1</sup>Department of Mechanical Engineering, Southern Taiwan University of Science and Technology, Tainan 71005, Taiwan

**Received:** 18 November 2020

**Accepted:** 8 January 2021

**Published online:**  
3 February 2021

© The Author(s), under exclusive licence to Springer Science+Business Media, LLC part of Springer Nature 2021

## ABSTRACT

This work utilized the optical properties of indium tin oxide/silver/indium tin oxide electrodes to set up the fitting range for spectroscopic ellipsometry (SE) analysis. Then, the SE fitting on the thickness and optical constants of each layer in several separate stages was investigated. In this way, the results suggest that the SE fitting can be able to converge rapidly and obtain the precise thickness of each layer. Experiment analysis shows that when the silver layer thickness was 8.5–11.5 nm, the sheet resistance of the uniform electrodes was  $< 8.5 \Omega/\text{sq}$ , while the average transmittances were  $> 82.0\%$  in the visible light region; the related Haacke indexes were  $> 22.0 \times 10^{-3} \Omega^{-1}$ . For photovoltaic application, when the silver layer thickness was 7.5–8.5 nm, the sheet resistance of the three-layer electrodes was  $< 9.0 \Omega/\text{sq}$ , while their average transmittance was  $> 77.5\%$ ; the related Haacke indexes were  $> 9.0 \times 10^{-3} \Omega^{-1}$ . Comparing the SE results with experimental measurements, it is concluded that the uniformity of the silver layer and the stability of the sputtering system were the major factors affecting the optoelectronic performance of the three-layer electrodes.

## 1 Introduction

Currently, indium tin oxide (ITO) thin film is the most widely applied material for transparent electrodes because of its perfect balance between high electrical conductivity and high transmittance [1]. Since ITO can be easily deposited into a thin film, it has wide applications, such as flat panel displays, electric heaters, smart windows, and thin film photovoltaics, etc. Moreover, along with the coming of large area, flexible, and energy saving optoelectronic

products, higher requirements are set for transparent electrodes. However, if we want the sheet resistance of these transparent electrodes to be under  $10.0 \Omega/\text{sq}$ , their thickness will exceed 300 nm, which will significantly weaken the optical quality of the transparent electrodes. In addition, the ITO is a member of ceramic materials whose brittleness is not suitable for flexible optoelectronic products. To solve these problems, the industrial world has made great efforts to develop various novel materials for transparent electrodes. Currently, technologies to take the place

Address correspondence to E-mail: kemo@stust.edu.tw

of ITO technology include metal mesh [2, 3], silver nanowires [4], carbon nanotube [5], graphene [6] conductive polymer [7], and multilayer electrodes [8–10]. Among them, combining the advantages of different materials, the technology of oxide/metal/oxide multilayer electrodes not only overcomes the counteracting optoelectronic properties between traditional transparent conductive materials, but is also compatible with existing manufacturing procedures. Thus, this technology is highly valued by industrial and academic circles.

To enhance the transmittance and reduce the sheet resistance of the electrodes at the same time, Ferhati et al. [8] used the particle swarm optimization technique to optimize the geometric structure of multilayer ITO/silver (Ag)/ITO and verified this with experiments. Study results show that light management could be improved by adjusting the thickness of silver and ITO layers. From their experiment on zinc oxide/aluminum/copper/zinc oxide flexible multilayer film, Wang et al. [9] found that the optical and electrical properties of flexible electrodes depended on the properties of the metal in the middle layer. An aluminum layer could help the flexible electrode to maintain its high transmittance since it had less influence on transmittance than a copper layer. On the other hand, a copper layer controlled the sheet resistance of the flexible electrodes. Our earlier study [10] also showed that the optoelectronic properties of the three-layer electrodes were decided by the quality of the intermedia silver layer, especially by controlling the thickness of the silver layer. A difference of merely 1 or 2 nm in thickness clearly affects the performance of the entire electrode.

Spectroscopic ellipsometry (SE) technology is widely favored by the industry world, not only because it is highly sensitive, highly precise, and non-destructive, but also because it can rapidly measure the thickness and optical constants of samples [11–15]. After analyzing the strengths and drawbacks of ellipsometry technology, Vedam [11] suggested five judgment rules: physical principles must be observed; the estimated value of mean square error (MSE) should be low; the fitting and measured curves should match with each other; the confidence limit of variable parameters should be small, and the correlation coefficient of fitting parameters should be low. Moreover, SE technology is not a direct measurement, but an inverse problem. And such problems are usually ill conditioned. Therefore, establishing an

appropriate SE model is very important for solving such problems.

Jung [16] used Drude and Lorentz model to estimate the optical constants of ITO film prepared under different sputtering conditions. He reported using a two-layer structure to simulate the gradient property of ITO film and found that the refractive index of ITO film was mainly affected by the orientation of crystalline. The more obvious the preferred orientation, the higher the refraction. He also found that the dissipation coefficient was affected by crystallinity and carrier concentration. Synowicki [17] believed that the structure of ITO film was quite complicated. It was not the only gradient but also could absorb a part of the incident light. The optical properties of the ITO film changed easily due to the sputtering and annealing conditions. Thus, he suggested using Cauchy model to obtain the refractive index and film thickness of ITO film in the visible light region. For measurement in other wavelength ranges, the gradient model and the Lorentz model would be more suitable. Furthermore, if SE analysis was combined with transmittance analysis, more precise solutions could be obtained.

As mentioned above, the quality and thickness of the metal intermediate layer are the key factors that determine the performance of the three-layer electrode. Thus, to ensure the quality of the electrodes, we need to know how to control and measure the thickness of the metal layer and how to understand the correlation between the deposition parameters and film thickness. The application of SE technology can quickly obtain the thickness of each electrode layer, but in addition to the complex optical properties of ITO itself, the problem that part of the light was absorbed by metal must be overcome [18]. Furthermore, because many parameters are used in the SE model of the three-layer electrode, it is not easy for the SE fitting to converge.

In this study, we plan to overcome the above issues and propose a method to analyze how deposition parameters affect the uniformity and thickness of the silver film. The proposed methodology based on optical measurements will simplify the SE model and allow the SE fitting to converge effectively.

## 2 Preparation and characterization

Four sets of ITO/Ag/ITO electrodes were fabricated by using Radio frequency (RF) sputtering technique. Each set had four batches, and each batch had four samples. The deposition time of the silver layer varied in each batch. During the sputtering process, the samples were kept on a rotating holder whose rotation rate was controlled by a computerized programming system. For samples of set-1, the holder was fixed. But for the rest of the samples, the holder was rotated at a speed of 5 rpm. We expected that rotating the sample holder at a fixed rate would improve the uniformity of the film thickness. The fabrication process of three-layer electrodes was as follows: First, an ITO film, to be used as the bottom layer, was sputtered on the Corning® glass substrates under the following conditions. The substrate and the target were kept vertically apart from each other at a 50 mm distance. The Ar gas flow rate was 35 sccm; RF sputtering power was 90 W; and the working pressure was 1.3 Pa. The whole experiment was carried out under dry condition at room temperature. A 4-inch ITO ( $\text{In}_2\text{O}_3$  with 10 wt%  $\text{SnO}_2$ ) target was used for RF sputtering to deposit an ITO layer of approximately 50 nm thickness. The thickness of the ITO layer was controlled by the deposition time and measured by the SE technique. Next, a silver layer was deposited on ITO/glass by RF sputtering under the same conditions, except that the sputtering power was 50 W. Finally, the upper ITO layer was deposited on the Ag/ITO/glass with the same sputtering parameters as those of the bottom ITO layer.

The optical properties, including transmittance and reflectance spectra of the three-layer electrodes, were characterized by a spectrophotometer (Jacos V-670). The electrical properties were measured using a four-point probe station (Keithley 2420 source meter interfaced with C# application). The thickness of each layer was measured using a variable-angle spectroscopic ellipsometer (Woollam M-2000U). All measurements were performed in the wavelength range of 245–1000 nm. SE measurement was carried out after the sputtering of each layer was finished. To reduce measurement errors, each SE measurement was carried out at three different incident angles ( $60^\circ$ ,  $65^\circ$ , and  $70^\circ$ ). Data analysis was conducted by using the CompleteEASE™ software package. The least

squares fitting method was performed and MSE was calculated to evaluate the quality of the fitting results.

The Cauchy model describes the dispersion of the film refractive index as a slowly varying function of wavelength with an exponential absorption tail [19]. This model is suitable for solving the optical properties of various transparent films, with or without a slight absorption property. In addition, a Surface Roughness model and an Intermix layer were adopted to reflect the physical properties of the three-layer electrodes. The optical constants of the Surface Roughness model are composed of the optical constants of the top layer material and air. Similarly, the optical constants of the Intermix model are composed of the optical constants from the layer below and above in a 50–50% ratio [19].

## 3 Experimental results

### 3.1 Optical properties

Figure 1 shows transmittance (left) and reflectance spectra (right) of all three-layer electrodes. Each transmittance or reflectance curve was calculated from the average value of all four samples in the same batch. From Fig. 1 one can see that all samples showed similar optical behaviors between 300 and 700 nm. All the samples in this study had a quite wide range of high transmittance. Especially at wavelength range 450–700 nm, the transmittance was obviously over 80%. Furthermore, the longer deposition time of the silver layer increased its thickness and improved its conductivity. Therefore, the reflectance of the samples in the near infrared (NIR) region also increased. Since all the samples had high conductivity, obvious reflectance occurred in the NIR region (over 800 nm). The transmittance and reflectance spectra of the set-3 samples in the NIR region were different from those of the samples of other sets. This was caused by the slow closing of the baffle during the sputtering process.

### 3.2 Fitting process of SE measurements

Based on the above measurement results, we assumed that the three-layer electrode should be transparent at 450–700 nm. Thus, the Cauchy model mentioned in the last section is suitable for describing the optical properties of this kind of electrode.

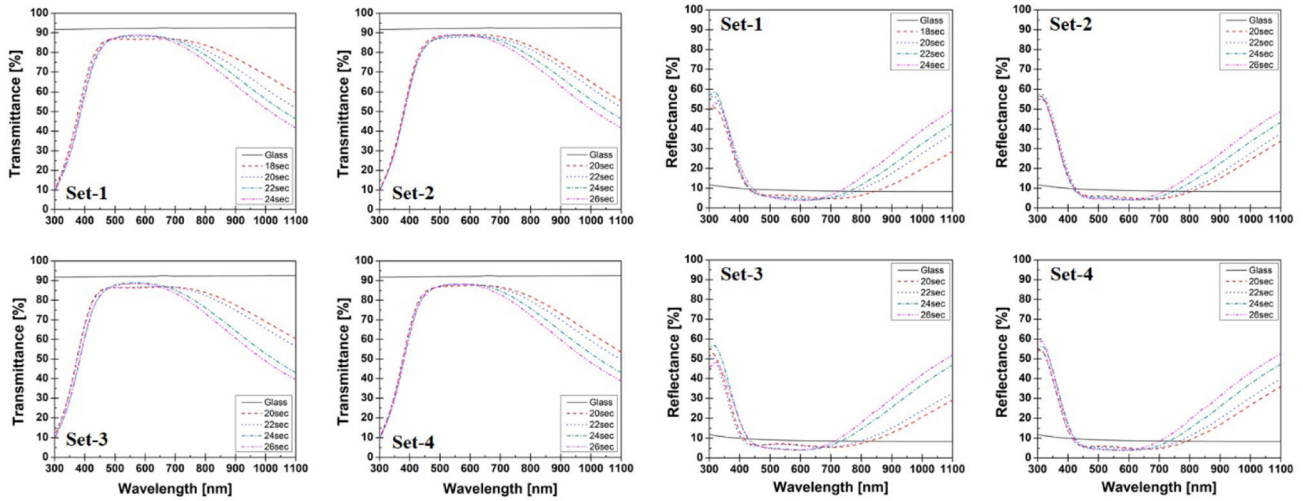


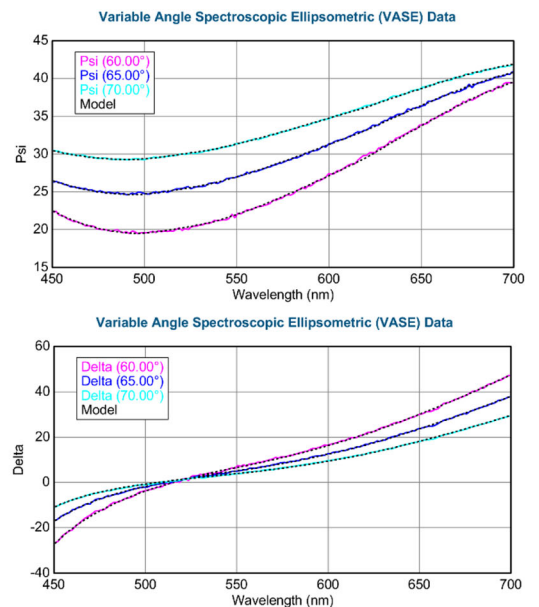
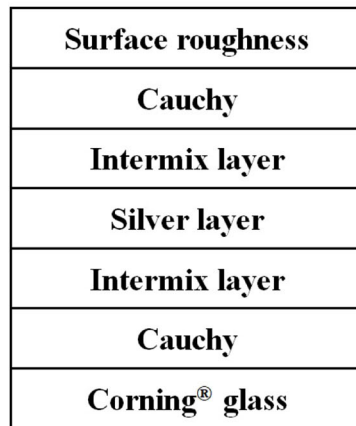
**Fig. 1** Transmittance (left) and reflectance (right) spectra of the three-layer electrodes. All samples showed similar optical behaviors between 300 and 700 nm. The longer sputtering time

of the silver layer led to an increase in the reflectance of the samples in the NIR region

Figure 2 is the optical model used in the SE fitting processes. In this SE model, the optical constants of the silver layer are built-in data in CompleatEASE™, while the optical constants of the glass substrate were based on our measurements. The SE fitting steps for the three-layer electrode were as follows. First, the Cauchy model of the bottom ITO layer was established on the substrate. In this fitting process, the thickness of the ITO layer and all optical constants were fitted one by one. The fitting result was saved as a file named “Layer-1 model.” In the second fitting stage, the SE measurement of the two-layer

structured Ag/ITO was used. Layer-1 model was used as the optical model of the bottom layer. All parameters of the Layer-1 model were fixed first. An Intermix layer was added onto Layer-1, and the optical model of the silver layer was also added for fitting. We first fitted the thicknesses of Ag and Intermix layer together and then all optical constants of the Layer-1 one by one. Nevertheless, the thickness of the Layer-1 was still fixed. After the fitting was finished, the result was saved as “Layer-2 model.” As such, the fitting of the thickness of a two-layer structure was completed. The establishment of the

**Fig. 2** Optical model for SE analysis (left), the typical results of SE analysis in this study (right)



fitting model for ITO/Ag/ITO film was similar to the second step. In the third stage, the SE measurement for ITO/Ag/ITO film was first introduced. The Layer-2 model was chosen as the optical model of the bottom layer. Likewise, all the parameters of the Layer-2 model were fixed first. Another Intermix layer was added to the silver layer. Then another Cauchy model was built on the Intermix layer to simulate the optical properties of the upper ITO layer. In this stage, we first fitted the optical constants and thickness of the ITO layer and then the thickness of the Intermix layer and the Surface Roughness layer one by one. Finally, we fitted the optical constants of the Layer-2 model one by one. As such, the fitting of a three-layer electrode was completed.

According to the optical properties of the three-layer electrode, we changed the fitting wavelength range to 450–700 nm from the 400–1000 nm in our early experiments, effectively enhancing the quality of the fitting results. Figure 2 (right) is a typical fitting result in this study. The fitting data was quite consistent with the measured data.

Figure 3 left shows the MSE values of all samples. The MSE values of the fitting results decreased from 5–10 to 3–7 after the fitting wavelength range was changed. The samples in set-1 (no rotation of holder) have uneven film thickness, and their MSE values show no obvious improvement. But, the samples in set-2–4 had uniform film thickness, and their MSE values reduced significantly, suggesting that the fitting quality was improved. As the silver layer thickness increased, the MSE values also increased slightly. This was mainly because more light was absorbed by the silver layer, causing the transparency to decrease.

The silver layer thickness in Fig. 3 (right) is obtained from SE analysis. After the change of fitting wavelength range and optimization of fitting steps,

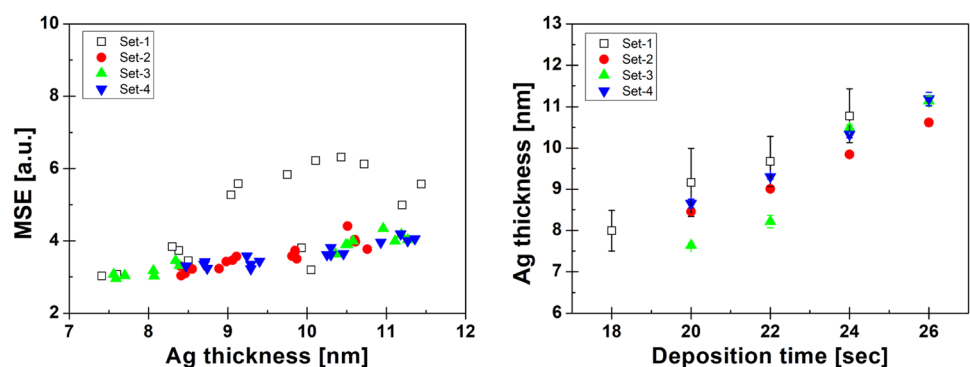
for samples with uniform thickness, their thicknesses showed no obvious differences from the earlier results although the MSE values decreased. However, for samples with uneven thickness, their thicknesses showed some differences. Besides, the standard deviation of the uneven thickness was 0.49–0.83 nm, while that of uniform thickness became smaller than 0.17 nm.

### 3.3 Optoelectronic performance

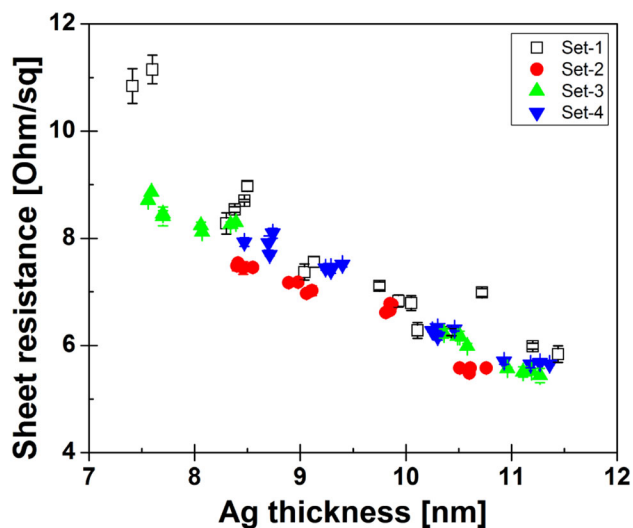
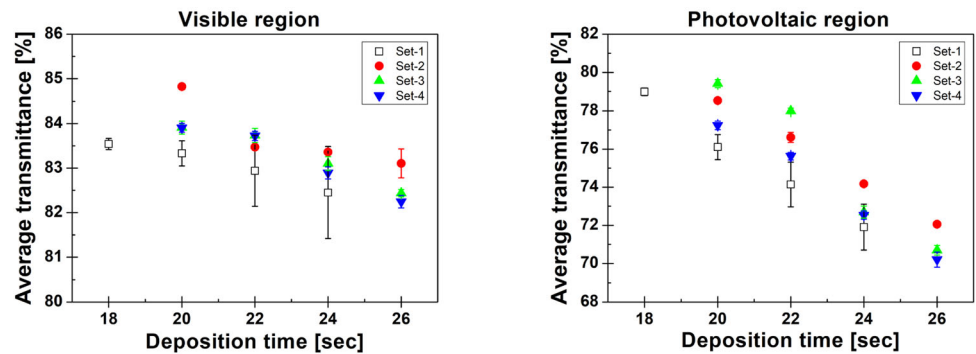
Figure 4 shows the average transmittances in the visible (380–760 nm) and photovoltaic (350–1100 nm) regions for all four batches of samples. As expected, the average transmittance in the visible range was maintained at over 83% until the deposition time of the silver layer was longer than 22 s. In general, the average transmittance decreased slowly with increasing deposition time. However, the three-layer electrodes could still yield an average transmittance slightly higher than those of pure ITO films in the visible region thanks to the anti-reflection of the upper metal oxide layer and the interference effects between the silver and ITO layers [10]. On the contrary, the average transmittance in the PV regions decreased immediately as the silver layer thickness increased. The main reason was that the rising carrier concentration caused by the increasing silver layer thickness, which in turn led to an increase of reflectance in the NIR region.

Figure 5 shows the sheet resistances of all samples. Similar to the average transmittance changes in the PV region, the sheet resistance decreased as silver layer thickness increased. This was also attributed to the rising carrier concentration when the silver layer became thicker, which in turn led to the increase of conductivity. Generally, the conductivity of films with uniform thickness is higher than films with the

**Fig. 3** MSE values of all fitting results (left), thicknesses of silver layer vs deposition time (right)



**Fig. 4** The average transmittance of all samples in visible light region (left) and PV region (right)



**Fig. 5** Sheet resistance of all samples

same but uneven thickness. Except for two samples in set-1, the sheet resistance of all the other samples was lower than  $10.0 \Omega/\text{sq}$ . This result is in good agreement with those of our earlier experiments [10]. That is, when the silver layer was thicker than 8.5 nm, all the samples had low sheet resistance. This means that all the samples prepared in this study have quite good conductivity.

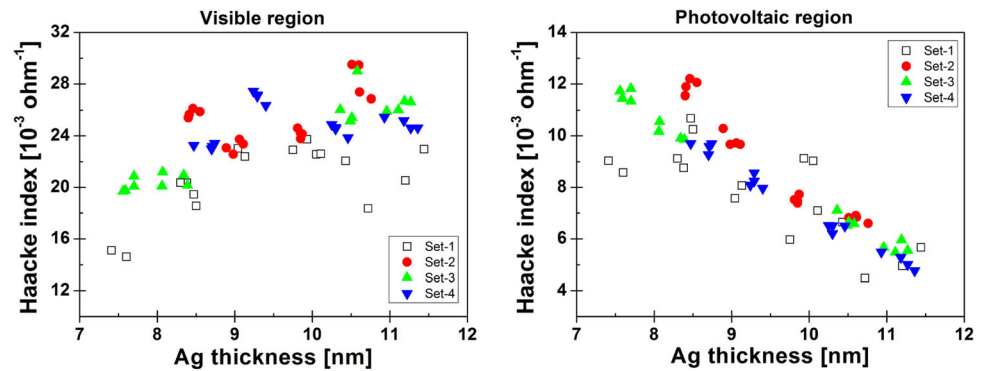
It can be concluded from the above measurements that all the samples maintained high transmittance when the silver layer was  $< 10.0$  nm. But the sheet resistance reduced as the silver layer became thicker. Thus, the best Haacke index should appear when the silver layer thickness is around 10.0 nm. In the PV region, on the other hand, both transmittance and sheet resistance decreased when the silver layer became thicker. Thus, the best Haacke index should appear when silver layer thickness locates at the beginning of the experimental range. From Fig. 6 (left), one can see that in visible light region, the

highest Haacke index appeared when the silver layer thickness reached 10.5 nm. When the silver layer thickness stayed homogeneously between 8.5 and 11.5 nm, the electrodes exhibited high and consistent optoelectronic properties. However, when the silver layer became thinner (or thicker, but the thicker one is not shown in Fig. 6), the Haacke index declined obviously. As to the Haacke index in the PV region, as expected, its highest values are located between 7.5 and 8.5 nm. The main reason was that the transmittance in the NIR region decreased significantly if the silver layer became too thick ( $> 8.5$  nm).

## 4 Discussion

This study utilized SE technology to precisely analyze the thickness of the silver layer and determine the connection between the thickness and optoelectronic properties of the ITO/Ag/ITO electrodes. By choosing a suitable wavelength range and optimizing fitting procedures, we effectively lowered the MSE values and enhanced the fitting preciseness. For optimizing fitting procedures, we applied Cauchy model to replace the dispersion equation, which is more physically meaningful. Subsequently, the fitting process rapidly converged and the precise thickness could be obtained. However, the preciseness of the optical constants of the three-layer electrodes was slightly compromised. Besides, fewer fitting parameters were needed when the fitting was conducted in several stages than in simultaneity. Meanwhile, we also presumed that the bottom layer thickness was not affected during the sputtering process. An inter-layer was used to describe the transition phenomena between layer and layer. The established SE model (Fig. 2 left) could clearly describe the optical behaviors of the three-layer electrodes (Fig. 2 right). It also

**Fig. 6** Haacke index of all samples in visible light region (left) and PV region (right)



enabled us to obtain the thickness of each layer effectively and rapidly. This enabled us to analyze the relationship between the deposition parameters and the performance of the electrodes.

From the thicknesses of the silver layers obtained from SE analysis, one can find that under the same deposition time, the thicknesses of the uneven silver layers might have a difference of more than 1.0 nm. However, when the substrate was rotated during the sputtering process, the silver layer thicknesses of the samples in the same batch had a difference of less than 0.45 nm, see Fig. 3 (right). Moreover, for samples prepared in different batches, but under the same sputtering conditions, uniform silver layer thickness had a difference of  $< 1.0$  nm. The samples of 20 s and 22 s in set-3 had bigger fluctuations in their thickness because during the sputtering process the baffle was defected and opened slower than usual. If the silver layer thickness was uneven, the conductivity of the silver layer was compromised. That is, sheet resistance increased, and subsequently, Haacke index decreased.

The thickness of the silver layer is the key factor affecting the optoelectronic properties of the three-layer electrode. From SE analysis on film thickness, one can see that when the thickness stayed at thinner than 10.0 nm, the electrode could still have a high transmittance. Also, the conductivity improved along with the increasing thickness. Thus, if we want to obtain high-performance three-layer electrodes in the visible light region, the silver layer thickness must be controlled at 10.0–11.0 nm. As for in PV region, a thicker silver layer caused high reflectance in the NIR region. Thus, silver layer thickness should be maintained at 7.5–8.5 nm so that high conductivity and high transmittance could be achieved at the same time. The sputtering experiment data for samples in

the same batch indicate that the standard deviation of silver layer thickness was 0.02–0.16 nm. But for samples in different batches, the standard deviation of their silver layer thickness was  $< 1.0$  nm.

## 5 Conclusion

In this work, a three-layer structure was used to prepare a high-performance transparent electrode whose optoelectronic properties included broadband transmittance. In order to obtain precise thickness measurements of each layer by using SE analysis, we utilized the wide-area transparent characteristics of the electrodes and the strength of the Cauchy model to conduct the SE fitting process. Then, the fitting of the thickness and optical constants for each layer in several separate stages was measured. In this way, we were able to have the fitting process converged rapidly and obtained the precise thickness of each layer. Analyses on the connection between the thickness of the silver layers and the optoelectronic properties of the electrodes showed that the silver layer had no obvious influences on the transmittance of the electrode when the silver layer thickness was at 7.0–10.0 nm. However, the silver layer thickness clearly affected the conductivity and transmittance in the PV region. In short, based on these data, we can determine the optimal silver layer thickness in visible or PV regions. For applications in the visible region, the optimal silver layer thickness was 8.5–11.5 nm. For applications in PV region, the optimal silver layer thickness was 7.5–8.5 nm. Analyses on the correlation of deposition parameters, silver layer thickness, and optoelectronic properties showed that uniform thickness promoted the conductivity of the electrodes. Furthermore, taking the sputtering system used in this study as an example, for samples

prepared under the same deposition conditions but in different batches, the biggest differences in their thickness were < 1.0 nm. This study shows that the proposed SE fitting procedure provided a rapid and precise measurement of the thickness of the three-layer electrodes. Our next study focus will be the development of a one-stage SE analysis procedure for in-line inspection.

## Acknowledgements

The authors gratefully acknowledge the financial support provided by the Ministry of Science and Technology of the Republic of China under Contact Number MOST 109-2221-E-218-001.

## References

1. K.L. Chopra, S. Major, D.K. Pandya, Transparent conductors—a status review. *Thin Solid Films* **102**(1), 1–46 (1983)
2. L. Hu, H. Wu, Y. Cui, Metal nanogrids, nanowires, and nanofibers for transparent electrodes. *MRS Bull.* **36**, 760–765 (2011)
3. J.-Y. Lee, S.T. Connor, Yi. Cui, P. Peumans, S.-P. Electrodes, *Nano Lett.* **8**(2), 689–692 (2008)
4. J. van de Groep, P. Spinelli, A. Polman, Transparent conducting silver nanowire networks. *Nano Lett.* **12**(6), 3138–3144 (2012)
5. J. van de Lagemaat, T.M. Barnes, G. Rumbles, S.E. Shaheen, T.J. Coutts, Organic solar cells with carbon nanotubes replacing In<sub>2</sub>O<sub>3</sub>: Sn as the transparent electrode. *Appl. Phys. Lett.* **88**, 233503 (2006)
6. J. Wu, H.A. Becerril, Z. Bao, Z. Liu, Y. Chen, P. Peumans, Organic solar cells with solution-processed graphene transparent electrodes. *Appl. Phys. Lett.* **92**, 263302 (2008)
7. J. Zou, H.-L. Yip, S.K. Hau, A.K.-Y. Jen, Metal grid/conducting polymer hybrid transparent electrode for inverted polymer solar cells. *Appl. Phys. Lett.* **96**, 203301 (2010)
8. H. Ferhati, F. Djeflal, A. Benhaya, Optimized high-performance ITO/Ag/ITO multilayer transparent electrode deposited by RF magnetron sputtering. *Superlattices Microstruct.* **129**, 176–184 (2019)
9. T.-y Wang, B.-J. Li, N.-F. Ren, L.-J. Huang, H. Li, Influence of Al/Cu thickness ratio and deposition sequence on photoelectric property of ZnO/Al/Cu/ZnO multilayer film on PET substrate prepared by RF magnetron sputtering. *Mater. Sci. Semicond. Process.* **91**, 73–80 (2019)
10. K.-M. Lin, R.-L. Lin, W.-T. Hsiao, Y.-C. Kang, C.-Y. Chou, Y.-Z. Wang, Effects of the structural properties of metal oxide/Ag/metal oxide multilayer transparent electrodes on their optoelectronic performances. *J. Mater. Sci. Mater. Electron.* **28**(16), 12363–12371 (2017)
11. K. Vedam, Spectroscopic ellipsometry: a historical overview. *Thin Solid Films* **313–314**, 1–9 (1998)
12. D.E. Aspnes, Expanding horizons: new developments in ellipsometry and polarimetry. *Thin Solid Films* **455–456**, 3–13 (2004)
13. D.E. Aspnes, Spectroscopic ellipsometry—past, present, and future. *Thin Solid Films* **571**, 334–344 (2014)
14. M. Losurdo et al., Spectroscopic ellipsometry and polarimetry for materials and systems analysis at the nanometer scale: state-of-the-art, potential, and perspectives. *J. Nanopart. Res.* **11**, 1521–1554 (2009)
15. E. Garcia-Caurel, A. De Martino, J.-P. Gaston, Li. Yan, Application of spectroscopic ellipsometry and Mueller ellipsometry to optical characterization. *Appl. Spectrosc.* **67**, 1–21 (2013)
16. Y.S. Jung, Spectroscopic ellipsometry studies on the optical constants of indium tin oxide films deposited under various sputtering conditions. *Thin Solid Films* **467**, 36–42 (2004)
17. R.A. Synowicki, Spectroscopic ellipsometry characterization of indium tin oxide film microstructure and optical constants. *Thin Solid Films* **313–314**, 394–397 (1998)
18. J.N. Hilfiker, N. Singh, T. Tiwald, D. Convey, S.M. Smith, J.H. Baker, H.G. Tompkins, Survey of methods to characterize thin absorbing films with spectroscopic ellipsometry. *Thin Solid Films* **516**, 7979–7989 (2008)
19. J.A. Woollam, Co., Inc. CompleteEASE™ Data Analysis Manual (2011)

**Publisher's Note** Springer Nature remains neutral with regard to jurisdictional claims in published maps and institutional affiliations.